Configurational entropy calculation of poly(α-alkyl β,L-aspartate)s **amorphous and crystalline films using gas permeation.**

L.F. del Castillo[1] , A. Andrio[2], J.A. Nava[1], S. Molla, S. Muñoz-Guerra[3] and V. Compañ[4,*].

[1]Departamento de Polímeros, Instituto de Investigaciones en Materiales, Universidad Nacional Autónoma de México. Ciudad Universitaria. Apartado Postal 70-360, Coyoacán, México DF, 04510.
[2]Departamento de Física. Escuela Superior de Tecnología y Ciencias Experimentales. Universitat Jaume I. 12072-Castelllón. (Spain).
[3]Departament de'Enginyeria Química, Universitat Politécnica de Catalunya. ETSEIB, Diagonal 647, 08028 Barcelona, (Spain).
[4]Departamento de Termodinámica Aplicada. ETSII. Universidad Politécnica de Valencia. Campus de Vera s/n. 46022-Valencia. (Spain).

(*) The whom correspondence to: V. Compañ. Universidad Politécnica de Valencia (Spain).
E-mail: vicommo@ter.upv.es

ABSTRACT

The permeability and diffusion coefficient of gases such as N_2, O_2 and CO_2 through two polymeric membranes of poly(α-alkyl β,L-aspartate)s (PAALA-n) were determined by the "time-lag" method. One of these membranes was crystalline (PAALA-1) and the other one was amorphous (PAALA-6). The comparison of the obtained result for both membranes is addressed by the calculation of the so called configurational entropy. The study has been done in the range of temperatures 20ºC to 70ºC.

KEY WORDS: Excess Configurational entropy, permeability, gas diffusion, amorphous polymer, crystalline polymer, poly(α-alkyl β,L-aspartate)s (PAALA-n).

1. INTRODUCTION

In the gas separation industry the use of polymeric membranes plays an important role, particularly in the separation of oxygen and nitrogen from the air to improve industrial combustion or to prevent oxidation. The same applies to the separation of hydrogen from hydrocarbon mixtures in refining processes. Then, it is of great interest to improve the efficiency of the membrane application in this area. The two properties that control the rate in the membrane operation are the sorption of a gas and the diffusion transport through the membrane. Both effects are separated according to the so called solution-diffusion model that consists of three steps: (1) Sorption (absorption or adsorption) upon the upstream boundary, (2) activated diffusion through the membrane, and (3) desorption or evaporation from the downstream boundary. Sorption (S) is a thermodynamic property depending on pressure and temperature, and ultimately on the molecular interactions parameter between the gas phase and the polymeric one. On the other hand, the diffusion transport coefficient (D) depends on the kinetic factors as the excess of free volume and the segmental-polymeric chain mobility. Considering also the desirable mechanical properties, the optimal materials proposed in the gas separation field are the vitreous ones, following the advances made in the last twenty years [1-2].

The gas operation efficiency depends on the permeability parameter (P), given by the product of the gas diffusion coefficient and the sorption. The gas-separation efficiency between two gases, named permselectivity, depends on the ratio of their permeabilities and is related to the difference of the gas activation energy and the gas activation entropy. For gases with similar diffusion coefficients the separation efficiency is given by the increase of the sorption coefficient. Actually, the presence of small nanoporous-structured fillers as zeolites, MOFs and porous silica can improve the efficiency of the operation and separation [3].

The development of new gas separation membranes is oriented to obtain a good balance of permeability and permselectivity. In order to improve these properties, a better knowledge of the relationship between chemical structure, thermodynamics and transport parameters is needed [4-8].

In this work we study the dependence of the permeability and diffusion coefficient with the temperature and the corresponding activation energy was obtained considering Arrhenius behavior. The permselectivity of the used gases is reported. As a matter of comparison between the results in the two mentioned polymeric materials, PAALA-1 and PAALA-6, the differences in the activation free energy and the activation entropy between crystalline and amorphous phases has been calculated, and then the configurational entropy is determinate. The results reported in the present

paper are completely new for the PAALA-6 while for PAALA-1 we are include date of new temperatures to complete the range 20ºC to 70ºC.

2. EXPERIMENTAL PART

a) Films preparation

Poly(α-alkyl β-L-aspartate), abbreviated PAALA-*n*, (*n* stands for the number of carbons contained in the alkyl side group) is a family of poly(β-peptide)s able to adopt regular folded arrangements similar to the well-known α-helix characteristic of proteins [9]. These polymers may be also considered as nylon-3 derivatives with an ester group stereorregularly attached to the β carbon atom of the main chain (Figure 1).

The structure and properties of PAALA-*n* have been systematically studied for a wide variety of *n* values within the range 1-22 [10]. PAALA-1 was prepared by the general procedure used for the synthesis of PAALA-*n* which is based on the non-assisted anionic ring-opening polymerization of the corresponding optically pure (*S*)-4-alkoxycarbonyl-β-lactams [11]. Specifically, (*S*)-4-methoxycarbonyl-β-lactam prepared from L-aspartic acid was polymerized in the presence of sodium pyrrolidone to render PAALA-1 in 82% yield [12]. Conversely, PAALA-6 was obtained by *trans*-esterification of poly(α-benzyl β,L-aspartate) with hexanol in the presence of titanium tetrabutoxide. The conversion of this reaction was 100% and the yield was around 85%. The structural characteristics and properties of these two PAALA's relevant with regards to the present work are given in Table 1. The PAALA films used for permeation experiments with a thickness of approximately 150-200 μm were prepared by hot-pressing in a Specac accessory (CTFM-P/N 15620). The average thickness of the membrane was calculated from five measurements using an electronic micrometer Deltascope MP10 manufactured by Fischer.

The structure of both PAALA-1 and PAALA-6 in the solid state has been recently studied by us using DSC, X-ray diffraction and modelling. PAALA-1 is highly crystalline and crystallizes in a pseudo-hexagonal lattice (a = 12.03 Å and c = 20.51 Å) made of right-handed 17/4 helices stabilized by intramolecular hydrogen bonds [23]. PAALA-6 chains are also arranged in helices, in this case of 13/4-type, which are packed in a hexagonal array but without tree-dimensional order; the hexyl side chains are unable to crystallize and they create an amorphous interhelical molten space that prevents the chains to be packed in a true crystal lattice. A scheme comparing the structures of PAALA-1 and PAALA-6 is depicted in Figure 2.

b) Permeation measurements

Permeation measurements of O_2, N_2 and CO_2 in the films were carried out in the experimental device schematically represented in Figure 3.

This usually consists of a classical device of double chamber of pressures (called upstream chamber and downstream chamber) coupled with the chromatography system used to analyzed mixture of gases. In this work the analysis was, so the gases keep pure from the bottles to the upstream chamber. The double chamber of pressures is immersed in a thermostatized bath controlled by a computer. Vacuum is applied to the system using a Leybold AG two-stage pump Trivac D 1,6 B able to reach $4x10^{-4}$ mbar. Pressures are measured using capacitive sensors. In the upstream chamber we use a Leybold DI 2000 sensor and in the downstream chamber we use a Tylan General CDHD45-11 sensor with an accuracy of 0.15% of reading. Valves are Nupro pneumatic valves model SS-4BK-1C. We control them from a computer using electro valves. A computer program is used to control temperature and pressure, to fill the gases reservoirs, and to measure pressures and calculate permeability and diffusion coefficient. This program repeats all these jobs for every temperature and pressure in the upstream chamber automatically.

Before each series of measurements, the system was vacuum calibrated by measuring the inlet of air into the downstream chamber. Keeping all the valves but 8, 1, 2, 3 and 4 closed, high vacuum (4 x 10^{-2} Torr) was made for 24 hours in both chambers. Then, valves 2 and 3 were closed and valve 5 was opened so the testing gas filled the 150 cm^3 deposit. We kept this gas there, inside a thermostated bath at a pressure close to that used in the experiment. The program computer suddenly closed valve 1 and opened valve 3 taking as zero this time. The evolution of the pressure in the downstream chamber with time was monitoring with the transducer pressure sensor CDHD45-11.

3. BACKGROUND

In the steady state the apparent permeability coefficient, P_{app}, can be written referred to standard pressure and temperature conditions as [14],

$$P_{app} = \frac{273}{76} \cdot \frac{V_b \cdot l}{A \cdot T \cdot p_a} \cdot \lim_{t \to \infty} \frac{dp_b(t)}{dt} \qquad (1)$$

where V_b, is the volume of the low pressure chamber, A the area of the membrane exposed to the flux, l is the membrane thickness, p_a the pressure of gas in upstream chamber, T the absolute

temperature in Kelvin and p_b the pressure of gas in the lowstream chamber with P_{app} usually expressed in barrers (1 barrer = 10^{-10} cm^3(STP) $cm/cm^2/s/cm$ of Hg).

The diffusion coefficient was obtained by the time-lag method and it is given by the intersection of the straight line *p* vs. *t* with the abscissa axis, such is shown in figure 4, using the equation suggested by Barrer [15]

$$D = \frac{l^2}{6\theta} \qquad (2)$$

where θ is the time-lag. The solution of diffusion coefficient by mean of eq.(2) assumes a constant diffusion coefficient and constant concentrations on both side of the membrane. In case in which the downstream chamber the pressure has a time dependent concentration the expression of eq.(2) should be corrected as Cruden and Meyyappan [16], and they show that the first correction of the time lag expression is twice in the Nguyen´s work [17], and in the linear approximation the right diffusion coefficient is given by

$$D = \frac{l^2}{6\theta}(1+\beta\theta) \qquad (3)$$

Where $\beta = -\frac{\partial \ln \Delta p}{\partial t}$. In this equation the usual time-lag is recovered at the steady state situation where β=0. The correction term $\beta\theta$ in eq.(3) means that diffusivities evaluated using time–lag method can have lower values than the real ones. As it was reported, considering the effect of the variation of the concentration on the diffusion coefficient obtained by equation 2, it has an uncertainty that it is by a factor of 3 [18].

According to the our methods, the relative error involved in the determination of the diffusion coefficient by the time-lag method, expressed in %, was obtained by the following expression,

$$\varepsilon(D) = 100 \cdot \left[\frac{2\varepsilon(l)}{l} + \frac{\varepsilon(\theta)}{\theta} \right] = 100 \cdot \left[\frac{2\varepsilon(l)}{l} + \frac{\varepsilon(n)}{n} + \frac{\varepsilon(m)}{m} \right] \qquad (4)$$

where $\varepsilon(l)$, $\varepsilon(n)$ and $\varepsilon(m)$ are the errors involved in the evaluation of the film thickness, (*l*), the slope (*m*), and interception (*n*), respectively. The permeability coefficient P_{app}, was obtained from the slope of the straight line of the *p* vs. *t* plot by means of the eq.(1). The precision of the permeability coefficient $\varepsilon(m)$, was estimated from the slope *m=dp/dt* of the isotherm in the long time conditions, and the correlation coefficient of the straight line *r*, according to the expression given in reference [19]. The precision obtained for the permeability were about 2-3% for all gases in all the films studied.

The product (*DS*) is defined as the apparent permeability coefficient P_{app}. It should be noted at this moment, that the apparent diffusion coefficient has also structural effects in a specific manner [19]. Then the apparent solubility coefficient can be obtained from the measurement of the apparent permeability and diffusion coefficients.

$$S_{app} = \frac{P_{app}}{D} \qquad (5)$$

This equation allows us obtaining the apparent solubility of the gas into the membrane.

4. RESULTS AND DISCUSSION

The As it is expected, the values of the permeability and diffusion coefficient obtained by the method of time-lag, for the two membranes under study, increase with temperature, as it can be seen in Figures 4 and 5. In addition, these values are bigger for the amorphous PAALA-6 films than for the crystalline PAALA-1, because of the amorphous structure of the former.

To see if the gas transport is a thermally activated process, we plotted the temperature dependence of the diffusion coefficient and apparent permeability parameters according to the Arrhenius expression:

$$X = X_0 \exp\left(-\frac{E_x}{RT}\right) \qquad (6)$$

In this equation, *X* represents the apparent permeability, diffusion or solubility coefficients, whereas X_0 are the corresponding pre-exponential factors and E_X the activation energies, per instance for the permeability coefficient, E_p, and for the diffusion coefficient, E_D. Consequently, activation energies associated with these processes may be determined from semi-logarithmic plots of *X* against 1000/*T*. Typical plots for the apparent permeability and diffusion coefficients of CO_2 are shown in Figures 4 and 5, respectively. From such plots, the values of E_p and E_D are obtained and they are given in Table 2. In general it follows the trends Ep (PAALA-1) > E_p (PAALA-6), while for E_D the trend is E_D (PAALA-1) < E_D (PAALA-6), for all gases studied. In short, the crystalline phase present in PAALA-1 films largely modifies the value of the diffusion coefficient compared to amorphous polymers PAALA-6; thus, at any temperature and for all gases (see figures 4, and 5), the diffusion coefficient in PAALA-1 is two orders of magnitude lower than PAALA-6 membranes.

Concerning to the configurational entropy in relation to the glass formation materials, it was defined as the difference of entropies of amorphous phase and the crystalline phase, and then the configurational entropy might be defined as [20-21]

$$\Delta S_c = S(glass\ \ phase) - S(crystal\ phase) \qquad (7)$$

In the present case, the identification of glass phase is the amorphous PAALA-6, and the crystal one is given by PAALA-1. The difference ΔS_C is able to obtain following the thermodynamic method, as given below.

As starting point consider the difference in the activation free energy for gas diffusion. In fact, the diffusion coefficient is related to the activation free energy according to the rate reaction model by Eyring and co-workers see reference [22]

$$D_{PAALA-1} = \frac{ekT}{h}(\lambda_{PAALA-1})^2 \exp\left(-\frac{G_{PAALA-1}}{RT}\right) = \frac{ekT}{h}(\lambda_{PAALA-1})^2 \exp\left(-\frac{E_{D1}}{RT} + \frac{S_{D1}}{R}\right) \quad (8)$$

$$D_{PAALA-6} = \frac{ekT}{h}(\lambda_{PAALA-6})^2 \exp\left(-\frac{G_{PAALA-6}}{RT}\right) = \frac{ekT}{h}(\lambda_{PAALA-6})^2 \exp\left(-\frac{E_{D6}}{RT} + \frac{S_{D6}}{R}\right) \quad (9)$$

where $G_{PAALA-i}$ is the free activation energy for the PAALA-1 (i=1) and PAALA-6 (i=6) respectively, E_{Di} is the activation energy and S_{Di} is the activation entropy for the PAALA-1 (i=1) and PAALA-6 (i=6). λ is the average jump length a penetrate molecule execute in one typical diffusive jump, *k* and *h* are the Bolztmann´s and Planck´s constants, respectively.

The free energy difference ΔG_D^{++} of each phase (amorphous and crystalline), was used in equations 8 and 9 in the following way:

$$\Delta G_D^{++} = G_{PAALA-1} - G_{PAALA-6} = (E_{D1} - E_{D6}) - T(S_{D1} - S_{D6}) = \Delta E_D - T\Delta S_D \quad (10)$$

Then, the ratio $\frac{D_{PAALA-1}}{D_{PAALA-6}}$ is related to the free energy difference ΔG_D^{++} of each phase (amorphous and crystalline), in the following way:

$$\Delta G_D^{++} = -R \cdot T \cdot \ln\left(\frac{D_{PAALA-1}}{D_{PAALA-6}}\left(\frac{\lambda_{PAALA-6}}{\lambda_{PAALA-1}}\right)^2\right) \quad (11)$$

To evaluate the excess of free energy according to eq.(11) the parameter λ should be evaluated first. Then, taking into account that this is the distance from one concentration in equilibrium position to another, it may be established for polymers by seeking the holes in the separation of polymeric chains. In figure 6 a model for determination of this parameter in PAALA-1 and PAALA-6 is given.

That consider a portion of the unit cell (see figure 2), as the unit of hexagonal cell for PAALAs was reported previously [23] [24]. Furthermore, it is known from the X-ray measurement that for these samples the first unit cell parameter (a) coincides with the diameter (2d) of the backbone of the polymers [25]. So that,

$$\lambda = 2d \cdot tg\,30. \qquad (12)$$

Where 2d is the diameter of the polymeric backbone with the alkyl side chain included.
The mean value of 2d for PAALA-1 is about 12.6Å [26] and 14.15Å for PAALA-6 [27]. Therefore, using equation (12) the mean jump length for each polymer are $\lambda_{PAALA-1} = 6.94\text{Å}$ and $\lambda_{PAALA-6} = 8.16\text{Å}$.

Using those values in equations 11, we plot ΔG_D^{++} versus T, and obtain a straight line, with the difference of activation energy as the crossing point at the origin and the difference in activation entropies as the slop. In fact, figure 7 the quantity ΔG_D^{++} versus temperature is given for three gases used namely carbon dioxide, oxygen and nitrogen, respectively. In this figure it is shown that their behaviour with temperature is linear, and as it can be seen in equation 11, the argument of the logarithm, the ratio $\frac{D_{PAALA-1}}{D_{PAALA-6}} \cdot 1.38$, maybe not an appreciable dependence with temperature, So that, there are two constants; they are the intercept and the slope of the straight line, which are related with the excess of activation energy and excess of entropy, respectively, of the two PAALAs polymers. In table 3 we can see the obtained values.

Note that, in this model the jump length is independent on the size of the gas molecular diameter, but does not the difference in activation energy and the activation entropy. Particularly, the change of entropy shows the loss of internal degrees of freedom [28] of the molecules when rotate across to the activated state; the trends is followed

$$\left(S_1 - S_6\right)_{CO_2} > \left(S_1 - S_6\right)_{N_2} > \left(S_1 - S_6\right)_{O_2} \qquad (13)$$

This trend denotes the difficulty of a molecular gas to jumpy barriers with different structural organization, from one side to the other, involving their rotational movement. Particularly, the larger differences between the results of the entropies are obtained for the CO_2.

On the other hand, the permselectivity of the polymeric films is usually expressed in terms of an ideal separation factor, α (A/B), which is equal to the ratio of the apparent permeability coefficient of the two gases considered.

$$\alpha\left(\frac{A}{B}\right)=\left(\frac{P_A}{P_B}\right)=\beta\left(\frac{A}{B}\right)\cdot\left(\frac{S_A}{S_B}\right) \qquad (14)$$

Where

$$\beta\left(\frac{A}{B}\right)=\left(\frac{D_A}{D_B}\right)\cdot \qquad (15)$$

Accordingly, values of the selectivity coefficient of CO_2 respect to O_2 and N_2 in the films used in this study are shown in Table 4. An inspection of these results shows that for example, the value of α (CO_2/N_2) = 1.9 in PAALA-1 films at 25°C increases up to 16.3 in PAALA-6 films. As expected, an increase in temperature tends to decrease the permselectivity of the amorphous films, also in crystalline polymers the permselectivity and diffusivities decrease when temperature increases. However when we compare the diffusivities of gas pair β(CO_2/O_2) and β(CO_2/N_2), we observe that the former is about four times bigger than the last in case of crystalline PAALA-1 (see table 5). The opposite happen when we compare the values of the permselectivity. These values for both pair CO2/O2 and CO2/N2 for crystalline PAALA-1 increases respect to the amorphous PAALA-6, since the crystallites also restrict amorphous chain mobility and increase the effective path length.

On the other hand, the obtained results for the apparent solubility are given in table 5, they follow the trend S_{app}(PAALA-6)> S_{app}(PAALA-1). For example, at 45ºC, the apparent solubility for PAALA-6 is about seven to ten times bigger than the solubility of PAALA-1 when the gas permeates is CO_2. This result shows that for this gas the effect of the amorphous phase tends to increase the free volume of material where the solubility is possible and to increase the interaction between the permeate molecules and polymeric matrix. This is related with the change of solubility between the crystalline and amorphous membranes, and in our case associated to the difference of structural distribution of the chains.

CONCLUSIONS

This article presents the results of permeation of three gases, O_2, N_2, and CO_2 in two polymeric membranes with different structures, one is crystalline and other is amorphous.

Diffusion coefficient and permeability measurements were carried out using the time-lag techniques. The apparent solubility and the permselectivity were evaluated by established methods and the results were discussed in relation to the structures of the samples under study. The activation energy and activation entropy were calculated using the expression of Eyring in the activated state theory. The difference of the activation energy between the non-crystalline PAALA-6 and crystalline PAALA-1 is related to the structural distribution of the polymeric chains, and is representative of the difference molecular distribution of them. The activation entropy was related to the loss of degrees of freedom when gas molecules jumps the barrier produced by the surrounding framework. The difference in the activation entropy for PAALA-1 and PAALA-6 gives the excess of configurational entropy and depends on the gas (see table 3).

ACKNOWLEDGEMENTS

This work was supported by the Dirección General de Investigación Científica y Técnica (DGICYT), Grant ENE-2011-Ref.24761 and also DGAPA-UNAM Proyecto IN 102512, and SEP-CONACYT 154626.

REFERENCES

1.Material Science of Membranes for Gas and Vapor Separation. Wiley Chichester UK 2006.

2 Vu D.Q., Koros W.J, *J. Membr. Sci*., **211**, 311 (2003)

3. Morre T.M, Koros W.J, *J Molec. Structure*, **739**, 87-98 (2005)

4. Ohya, H., Kudryavtsev, V.V., Semenova, S.I. *Polyimide Membranes*, Gordon and Breach Publishers: Tokyo, 1996.

5. Koros, W. J., Fleming, G. K. *J. Memb. Sci*., **83**, 1-80 (1993)

6. Stern, S.A. *J. Memb. Sci*., **94**, 1-65 (1994)

7. Al-Masri, M., Kricheldorf, H. R., Fritsch, D. *Macromolecules* **1999,** 32, 7853

8. Petropoulos, J. H., *Pure Appl. Chem*., **65** (2), 219 (1993)

9**.** Fernández-Santín, J. M., Aymamí, J., Rodríguez-Galán, A., Muñoz-Guerra, S., Subirana, J.A., *Nature (London)* **53**, 311-312 (1984)

10. Muñoz-Guerra, S., López-Carrasquero, F., Fernández-Santín, J. M., Subirana, J.A., In *Polymeric Materials Encyclopedia*, Salamone, J. C., Ed., CRC Press: Boca Raton, FL, 1996, Vol.6, p 4694-4700.

11. López-Carrasquero, F., García-Alvarez, M., Muñoz-Guerra, S., *Polymer*, **35**, 4502-4509 (1994)

12. García-Alvárez, M., López-Carrasquero, F., Tort, E., Rodríguez-Galán, A., Muñoz-Guerra, S., *Synth. Comm*. **24**, 745-753 (1994)

13. Doty, P., Bradbury, J.A., Haltzer, A.M., *J. Am. Chem. Soc*. **78**, 947 (1956)

14. Compañ, V.; López-Lidón, M.; Andrio, A.; Riande, E. Macromolecules 31 (1998) 6984.

15. Barrer, R.M. *Trans. Faraday Soc.* **1939**, 35, 628

16. Cruden, B.A., Meyyappan, M. J. Membr. Sci. 221 (2003) 47-51.

17. Nguyen, X.Q., Broz Zdenek, Uchytil, P., Nguyen, Q.T. J. Chem Soc. Faraday Trans, 88(24), (1192) 353-3560.

18. Rogers C. E. "Permeation of gases and vapors in polymers" in "Polymer Permeability" Ed. by Comyn J. Cap.2. Chapman and Hall, London 1985.

19. Compañ, V; del Castillo, L.F.; Hernández, S.I.; López-Gonzalez, M.M.; Riande, Evaristo. Journal of Polymer Science: Part B: Polymer Physics, Vol. 48, (2010) 634-642.

20. Donth, E. The glass transition, relaxation dynamics in liquids and disorder materials. Springer-Verlag. Berlin, 2001.

21. Angell, CA., Sare, J.M. J. Phys. Chem. 82 (1978) 2622-2629.

22. Glasstone, S.; Laidler, K. J.; Eyring, H. *The Theory of Rate Processes*; McGraw Hill Book Co., Inc.: New York, 1941.

23. Juan José Navas,CarlosAlemán, Francisco Lopez-Carrasquero and Sebastian Muñoz-Guerra. Polymer (1997) 38, 3477-3484

24. Zanuy D, León S. Alemán C, Muñoz-Guerra S.Polymer 41 (2000) 4169-4177.

25. Juan J Navas, Carlos Alemán, Francisco López-Carrasquero and Sebastian, Muñoz-Guerra. Macromolecules (**1995)**, 28, 4487-4494.

26. López-Carrasquero, F.; García-Alvarez, M.; Navas, J. J.; Alemán, C.; Muñoz-Guerra, S. Macromolecules (**1996)**, 29, 8452-8461

27. F. López-Carrasquero, S. Monserrat A. Martinez de Ilarduya and, S. Muñoz-Guerra, . Macromolecules (**1995)**, 28, 5535-5546.

28. Anshu Sing-Ghosal and W.J. Koros. Ind. Eng. Res (1999) 38, 3647-3654.

.

TABLES

Table 1. Some data of the PAALA-*n* used in this work

PAALA-*n*	R	$[\eta]$[a] (dL/g)	M_v[b] (g/mol)	T_m[c] (ºC)	ρ[d] (g/cm^3)
PAALA-1	$-CH_3$	2.88	$2.2\cdot10^5$	287	1.36
PAALA-6	$-CH_2CH_2CH_2CH_2CH_2CH_3$	2.62	$5.8\cdot10^5$	-	1.07

[a]ntrinsic viscosity measured in DCA at 25 ºC.
[b]Average molecular weight calculated on the basis of the equation reported for poly(γ-benzyl-L-glutamate) [13].
[c]Melting temperature measured by DSC.
[d]Density measured by flotation in a KBr aqueous solution.

Table 2. Activation energies in kcal/mol for the permeability and diffusion coefficients of carbon dioxide, oxygen and nitrogen Measurements in PAALA-1, PAALA-6 and films. The SD in the slope as calculated from [19], $\varepsilon(m) = m\frac{\tan(arc\cos(r))}{\sqrt{N-2}}$ where *N* is the number of experimental points used for the straight line determination and r the correlation coefficient.

Films	PERMEATION E_P (kcal/mol)			DIFFUSION E_D (kcal/mol)		
	CO_2	O_2	N_2	CO_2	O_2	N_2
PAALA-1	6.6±0.2	13.1±0.52	10.7±0.4	4.4±0.32	5.3±0.7	6.3±0.2
PAALA-6	4.6±0.2	7.1±0.2	7.0±0.2	8.1±0.3	8.8±0.3	8.8±0.2

Table 3. Values of the slopes and intercepts for each one where the variation of ΔG_D^{++} versus T is given. The SD in the slope and intercept as calculated from [19], by mean of the expressions: $\varepsilon(m) = m\frac{\tan(arc\cos(r))}{\sqrt{N-2}}$ and $\varepsilon(n) = \varepsilon(m)\sqrt{\frac{\sum_i x_i^2}{N}}$ where *N* is the number of experimental points used for the straight line determination and r the correlation coefficient of straight-line.

Gas	S_1-S_6 (cal mol^{-1} K^{-1})	E_1-E_6 (cal mol^{-1})
CO2	17.3±0.4	3800±200
O2	15.6±0.4	2800±200
N2	16.7±0.3	2500±200

Table 4. Permselectivities ($\alpha = \left(\frac{P_A}{P_B}\right)$) and diffusivities ($\beta = \left(\frac{D_A}{D_B}\right)$) of pair of gases for PAALA-1 and PAALA-6 polymers.

Sample	T (ºC)	α (CO_2/O_2)	α (CO_2/N_2)	β (CO_2/O_2)	β (CO_2/N_2)
PAALA-1	20	3.37	2.19	1,24	5.4
	25	2.44	1.94	1.10	4.6
	30	2.34	1.78	1.19	4.8
	35	1.91	1.15	1.30	5.1
	40	1.66	1.47	1.33	5.1
	45	1.68	1.19	1.22	4.6
	50	1.20	1.22	1.13	4.1
	55	1.06	1.12	1.07	3.8
	60	0.89	1.03	0.96	3.5
	65	0.60	0.73	1.02	3.6
	70	0.68	0.72	1.00	3.3
PAALA-6	20	8.55	19.73	0.51	0.83
	25	7.37	16.31	0.48	0.72
	30	7.37	19.89	0.52	0.81
	35	6.85	16.17	0.47	0.72
	40	7.14	15.53	0.53	0.79
	45	5.97	14.31	0.47	0.69
	50	5.77	12.43	0.53	0.77
	55	4.75	12.74	0.48	0.69
	60	4.81	12.52	0.49	0.68
	65	5.14	11.44	0.44	0.61
	70	4.70	10.68	0.54	0.74

Table 5.Coefients of apparent permeability, diffusivity and solubility of CO_2, O_2 and N_2 gases for PAALA-1 and PAALA-6 films at different temperatures.

Film	T (ºC)	P_{app} Barrer			$Dx10^9$ cm^2/s			$S_{app}x10^2$ $cm^3gas \cdot cm^{-3}polym\ cmHg^{-1}$		
		CO_2	O_2	N_2	CO_2	O_2	N_2	CO_2	O_2	N_2
PAALA-1	20	0.5	0.15	0.23	8.7	7.0	0.16	0.58	0.22	14
	25	0.66	0.27	0.40	9.0	8.2	0.20	0.73	0.33	17
	30	0.74	0.32	0.42	11.2	9.5	0.23	0.67	0.33	18
	35	0.76	0.40	0.66	14.2	10.9	0.28	0.53	0.37	24
	40	1.06	0.64	0.73	16.7	12.6	0.33	0.64	0.51	22
	45	1.26	0.75	1.06	17.6	14.4	0.39	0.71	0.52	27
	50	1.48	1.23	1.22	18.5	16.4	0.45	0.80	0.75	27
	55	1.57	1.49	1.41	20.0	18.6	0.52	0.78	0.80	27
	60	1.93	2.28	1.98	20.2	21.1	0.62	1.00	1.1	33
	65	2.29	3.83	3.12	24.2	23.7	0.70	0.95	1.6	45
	70	2.76	4.08	3.81	26.7	26.7	0.80	1.03	1.5	47
PAALA-6	20	47.1	5.51	2.39	79.4	155.3	96.0	5.9	0.35	0.25
	25	48.2	6.48	2.93	89.2	196.2	123.9	5.3	0.33	0.24
	30	66.6	9.04	3.35	127.6	246.2	158.4	5.2	0.37	0.21
	35	69.6	10.2	4.31	144.5	306.5	200.1	4.8	0.33	0.21
	40	83.6	11.7	5.38	199.0	379.0	253.2	4.2	0.31	0.21
	45	88.4	14.8	6.18	217.7	465.6	316.5	4.1	0.32	0.20
	50	102.2	17.7	8.22	302.0	568.1	393.1	3.3	0.31	0.21
	55	110.6	23.2	8.68	335.0	689.0	485.1	3.3	0.34	0.18
	60	119.8	24.9	9.57	403.0	830.7	594.2	3.0	0.30	0.16
	65	136.6	26.5	11.9	441.1	996.5	794.3	3.1	0.27	0.16
	70	146.3	31.1	13.7	645.7	1188	876.8	2.3	0.26	0.16

FIGURE CAPTIONS

FIGURE 1. Chemical formula of PAALA-*n*.

FIGURE 2. View along the *c*-axis (chain axis) of the packing of chains in PAALA-1 and PAALA-6.

FIGURE 3. Experimental set-up used in the gas transport measurements. M: membrane. Numbers 1 to 15 valves. Grey colour indicates the thermostatized. area of the system The deposit of volume 150 cm^3 is introduced into the thermostatized bath to fix the temperature of the gases before start the experiment.

FIGURE 4. Values of lnD versus 1000/*T*, for PAALA-1 (■) and PAALA-6 (●) for the gas CO_2, with time-lag the method.

FIGURE 5. Values of lnP versus 1000/*T*, for PAALA-1 (■) and PAALA-6 (●) for the gas CO_2, with time-lag method.

FIGURE 6. Representative model of part of the hexagonal cell of PAALA-1 and PAALA-6 (see figure 2) for determination of the mean jump length of molecules of diffusion-gas.

FIGURE 7. Free energy difference $-\Delta G^{++}$ vs. T for carbon dioxide (■), oxygen.(●) and nitrogen (◆) .

FIGURES

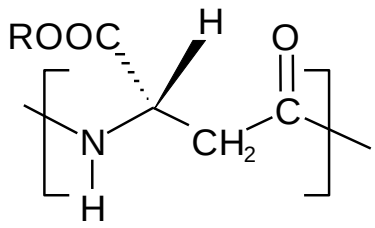

FIGURE 1. Chemical formula of PAALA-*n*.

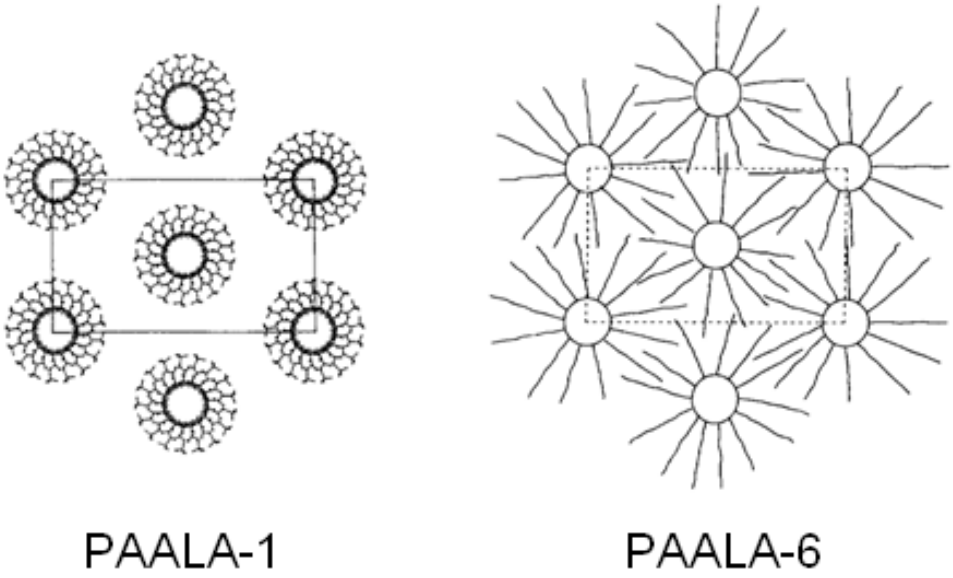

FIGURE 2. View along the *c*-axis (chain axis) of the packing of chains in PAALA-1 and PAALA-6.

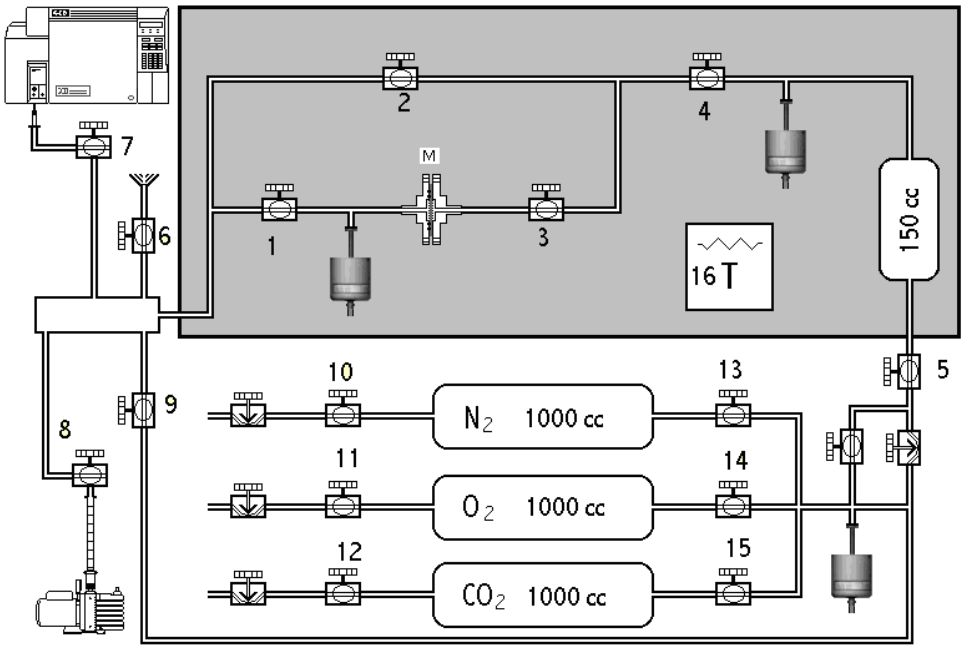

FIGURE 3. Experimental set-up used in the gas transport measurements. M: membrane. Numbers 1 to 15 valves. Grey colour indicates the thermostatized. area of the system The deposit of volume 150 cm^3 is introduced into the thermostatized bath to fix the temperature of the gases before start the experiment.

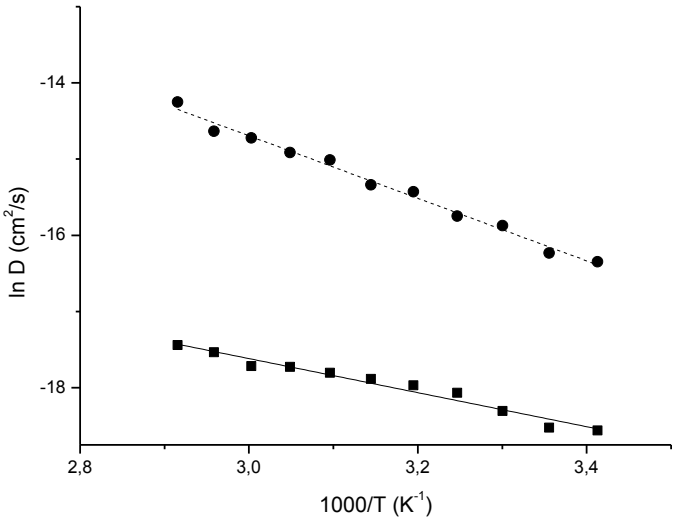

FIGURE 4. Values of lnD versus 1000/*T*, for PAALA-1 (■) and PAALA-6 (●) for the gas CO_2, with time-lag the method.

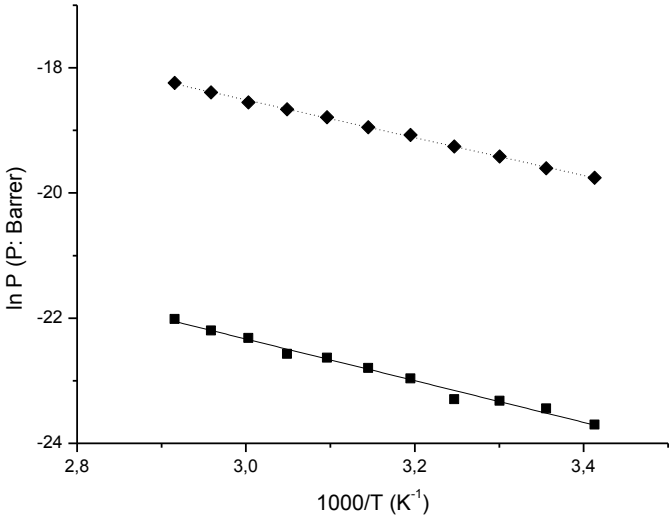

FIGURE 5. Values of lnP versus 1000/*T*, for PAALA-1 (■) and PAALA-6 (●) for the gas CO_2, with time-lag method.

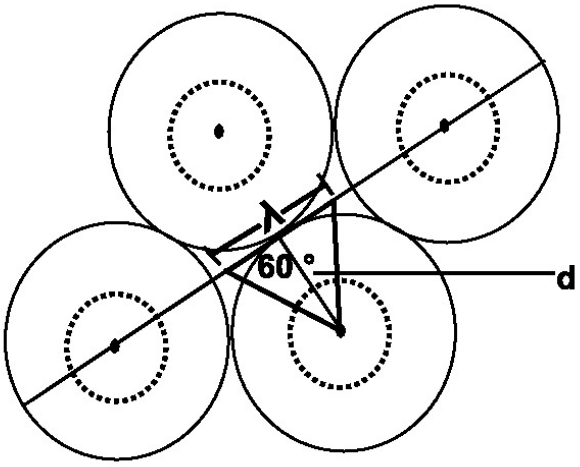

Figure 6. Representative model of part of the hexagonal cell of PAALA-1 and PAALA-6 (see figure 2) for determination of the mean jump length of molecules of diffusion-gas.

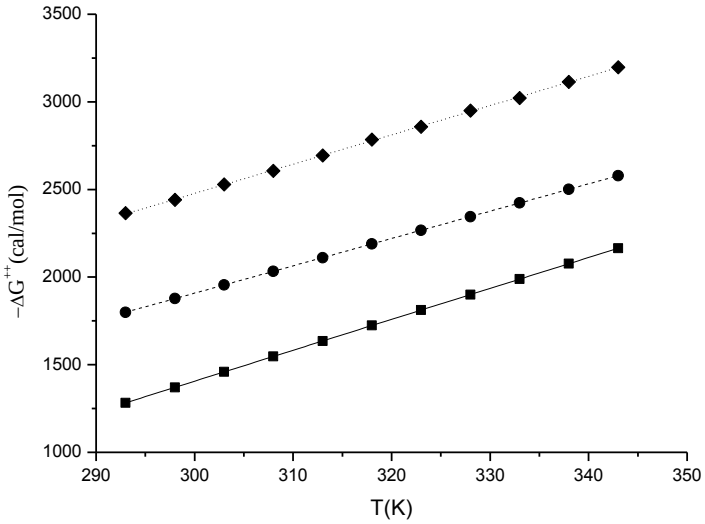

FIGURE 7. Free energy difference $-\Delta G^{++}$ vs. T for carbon dioxide (■), oxygen (●) and nitrogen (◆) .